ACS APPLIED MATERIALS & INTERFACES

Research Article

www.acsami.org

Interplay of Substrate Conductivity, Cellular Microenvironment, and Pulsatile Electrical Stimulation toward Osteogenesis of Human Mesenchymal Stem Cells in Vitro

Greeshma Thrivikraman,[†,§,⊥] Poh S. Lee,[†,⊥] Ricarda Hess,[†] Vanessa Haenchen,[†] Bikramjit Basu,[*,‡] and Dieter Scharnweber[*,†]

[†]Max Bergmann Center of Biomaterials, Technische Universität Dresden, Budapester Straße 27, 01069 Dresden, Germany

[‡]Laboratory for Biomaterials, Materials Research Centre, Indian Institute of Science, Bangalore 560012, India

[§]Centre for Nano Science and Engineering, Indian Institute of Science, Bangalore 560012, India

Supporting Information

ABSTRACT: The influences of physical stimuli such as surface elasticity, topography, and chemistry over mesenchymal stem cell proliferation and differentiation are well investigated. In this context, a fundamentally different approach was adopted, and we have demonstrated the interplay of inherent substrate conductivity, defined chemical composition of cellular microenvironment, and intermittent delivery of electric pulses to drive mesenchymal stem cell differentiation toward osteogenesis. For this, conducting polyaniline (PANI) substrates were coated with collagen type 1 (Coll) alone or in association with sulfated hyaluronan (sHya) to form artificial extracellular matrix (aECM), which mimics the native microenvironment of bone tissue. Further, bone marrow derived human mesenchymal stem cells (hMSCs) were cultured on these moderately conductive (10^{-4}–10^{-3} S/cm) aECM coated PANI substrates and exposed intermittently to pulsed electric field (PEF) generated through transformer-like coupling (TLC) approach over 28 days. On the basis of critical analysis over an array of end points, it was inferred that Coll/sHya coated PANI (PANI/Coll/sHya) substrates had enhanced proliferative capacity of hMSCs up to 28 days in culture, even in the absence of PEF stimulation. On the contrary, the adopted PEF stimulation protocol (7 ms rectangular pulses, 3.6 mV/cm, 10 Hz) is shown to enhance osteogenic differentiation potential of hMSCs. Additionally, PEF stimulated hMSCs had also displayed different morphological characteristics as their nonstimulated counterparts. Concomitantly, earlier onset of ALP activity was also observed on PANI/Coll/sHya substrates and resulted in more calcium deposition. Moreover, real-time polymerase chain reaction results indicated higher mRNA levels of alkaline phosphatase and osteocalcin, whereas the expression of other osteogenic markers such as Runt-related transcription factor 2, Col1A, and osteopontin exhibited a dynamic pattern similar to control cells that are cultured in osteogenic medium. Taken together, our experimental results illustrate the interplay of multiple parameters such as substrate conductivity, electric field stimulation, and aECM coating on the modulation of hMSC proliferation and differentiation in vitro.

KEYWORDS: *polyaniline, mesenchymal stem cells, osteogenic differentiation, collagen, sulfated hyaluronan, transformer-like coupling, electric fields*

1. INTRODUCTION

The inventive approach of using biomaterial properties to influence mesenchymal stem cell differentiation is considered as an attractive strategy in bone tissue engineering.[1] Several physicochemical cues such as roughness, porosity, topography, as well as chemical composition are reported to induce mesenchymal stem cell differentiation toward osteogenic lineages.[2,3] Apart from material properties, physical signals are also proven as potent osteogenic stimulators.[4] Such understanding on various physicochemical factors that govern osteogenesis is essential to establish appropriate in vitro culture conditions, thus improving cellular response and direct a desired outcome.[5] For instance, reports suggest the overriding potential of substrate's physical properties in eliciting cellular effects against the traditional induction method using medium supplements that are not physiologically relevant.[6,7]

The existence of endogenous electric field within bone tissues, and its role in bone physiology, has strengthened the notion among scientists that applying electric stimulation externally can also elicit osteogenic differentiation of stem/

Received: July 15, 2015
Accepted: September 29, 2015
Published: September 29, 2015

DOI: 10.1021/acsami.5b06390
ACS Appl. Mater. Interfaces 2015, 7, 23015–23028

progenitor cells and bone formation in vitro.[8,9] On these grounds, human mesenchymal stem cells (hMSCs) exposed to alternating current (A.C.) electric field (EF) induced higher osteogenic marker expression and stress response, followed by accelerated differentiation.[10] Besides, various forms of EF stimulation are recognized clinically as an effective and noninvasive method for enhancing bone healing and treating fracture nonunion.[11] Specifically, exposure to EF results in the activation of charged transmembrane receptors involving the calcium/calmodulin pathway, which increases TGF-β1 expression in osteoblasts.[12]

Among the numerous attempts to develop tissue interactive substrates, the use of electroactive polymeric biomaterials received wider attention, as it can deliver localized electrical stimulus, hence allowing precise spatial control of stimulation.[13] In addition to electrical conductance, its versatility provides the additional benefit of incorporating specific biological moieties to recapitulate the native extracellular matrix.[14] Among the most investigated conducting polymers, polyaniline is regarded as suitable cell culture platforms by virtue of its biocompatibility, good environmental stability, and also its competency to be electrically switched between conductive and resistive states.[13] Osteoblasts grown on nanocomposites created from aniline oligomers and poly(lactic-*co*-glycolic acid) blends exhibited improved proliferation and differentiation, when exposed to external electric pulse stimuli.[15]

Immobilizing extracellular matrix (ECM) biomolecules onto the surface of biomaterials are recognized as one of the most suitable strategies to mimic native tissue microenvironment and to improve biocompatibility. As one of the major organic component of bone extracellular matrix, collagen type I (Coll) is often coated on implants and was reported to have a positive effect in promoting adhesion, proliferation, and differentiation of osteoblasts.[16] Likewise, incorporating additional components, such as sulfated hyaluronan derivatives (sHya), further enhances osteoblastic adhesion and osteogenic differentiation since they are known to specifically bind positively charged amino acid sequences of the growth factors, thereby modulating their activity.[17,18]

By applying pulsed EF stimuli of very low frequency by transformer-like coupling approach (TLC-PEF), Hess et al. could accomplish significant increase in ALP activity as well as in gene expression of osteogenic markers. This noninvasive stimulation technique nullifies the side effects that occur either due to the biochemical reactions or through magnetic field generated during field exposure.[19] The same group further validated that a combination of transformer-like coupling pulsed electric field (TLC-PEF) stimulation along with immobilization of matrix biomolecules, such as Coll and sHya, can augment osteogenesis.[20] While the importance of low frequency pulsed electric field driven osteogenesis is well established, there is still a lack of profound understanding to know whether the desired osteogenic response can be regulated when grown on conducting biomaterial substrates.

In the above perspective, we assessed the proliferation and differentiation of hMSCs cultured on aECM modified conducting PANI substrates stimulated under TLC-PEF (denoted hereafter as PEF for brevity). Through this comprehensive investigation, we sought to elucidate the following objectives: (a) to determine the influence of underlying substrate conductivity in eliciting osteogenic response upon PEF stimulation and (b) to assess whether supplementation of highly sulfated hyaluronan (sHya) will further enhance osteogenesis of hMSCs in the presence of PEF. To address the first objective, hMSCs were grown on insulating glass coverslip (control/Coll) and on moderately conducting PANI substrates (PANI/Coll), which were concurrently exposed to PEF. The second objective was addressed by comparing the hMSCs grown on Coll coated PANI substrate with and without sHya immobilization.

2. MATERIALS AND METHODS

2.1. Biomaterial Substrate Fabrication. *2.1.1. Preparation of PANI Substrates.* The synthesis of PANI was based on the oxidation of aqueous solutions of aniline by ammonium peroxydisulfate at −30 °C.[21] To obtain thin films of PANI, 3.5 wt % of the PANI was added very slowly to N,N′-dimethyl propylene urea (DMPU) (Spectrochem Pvt. Ltd., India) at room temperature. The PANI solution was then centrifuged at 3000*g* for 5 min at room temperature to remove any undissolved aggregates. This solution was drop casted onto glass slides and placed in vacuum oven at 80 °C for 96 h to thoroughly remove the solvent. Free-standing films of thickness in the range of 100−300 μm were obtained by immersing these dried films coated on glass slides in deionized water for few minutes.

2.1.2. Artificial Extracellular Matrix (aECM) Coating on PANI Substrates. For protein immobilization onto the substrates, two ECM components, namely Coll (rat tail; BD Bioscience, Erembodegem, Belgium) and sHya with a degree of sulfation per disaccharide repeating unit of 3.0 (Innovent, Jena, Germany), were used.[22] Briefly, the sample surface was sterilized using 70% ethanol and washed with PBS twice. To coat the surface with Coll/sHya, Coll was diluted in 10 mM acetic acid to a final concentration of 1 mg/mL and mixed with equally concentrated sHya solubilized in sterile fibrillogenesis buffer, pH 7.4 (50 mM disodium hydrogen phosphate, 11 mM potassium dihydrogen phosphate). These samples are depicted as PANI/Coll/sHya in later sections. For coating without sHya, 1 mg/mL of Coll was mixed with an equal volume of fibrillogenesis buffer devoid of sHya, corresponding to a final concentration of 500 μg/mL. These samples are depicted as PANI/Coll in later sections. Additionally, glass coverslip was coated with Coll alone and is used as the baseline for comparison (control/Coll). Individual sample was coated with 1 mL of respective coating solution and allowed to fibrillate overnight at 37 °C. Subsequently, the samples were washed twice in deionized water and air-dried in sterile environment. When completely dried, they were sterilized by gamma irradiation with a standard dose of 25 kGy.

2.2. Physico-Chemical Characterization of aECM Coating. *2.2.1. aECM Morphology and Adsorption Behavior.* The chemical stability of the aECM coating on PANI substrates was determined directly after washing the coated samples twice in PBS and subsequent incubation for 1 h, 1 day, and 7 days in PBS at 37 °C. The amounts of Coll adsorbed to PANI/Coll and PANI/Coll/sHya substrates were evaluated by fluoraldehyde o-phthalaldehyde (OPA) assay (Thermo scientific) according to manufacturer's protocol. Briefly, the substrates were kept for 10 min at 100 °C for protein denaturation. Subsequently, each film was incubated overnight at 60 °C in 1 mL of digestion buffer (0.1 mg/mL collagenase A in TES buffer, 50 mM N-[Tris(hydroxymethyl)methyl]-2-aminoethanesulfonic acid, 0.36 mM $CaCl_2$, pH 7.4). From this, 20 μL of digest was added to 200 μL of 0.8 mg/mL OPA reagent, and the fluorescence intensity was measured in a microplate fluorescence reader (Tecan) with excitation at 340 nm and emission at 440 nm.

The concentration of incorporated sHya was quantified using 1,9-dimethylmethylene blue (DMMB) assay (Sigma).[23] Briefly, the samples were digested in 400 μL of papain solution (0.1 mg/mL) at 60 °C for 24 h, and 40 μL of digest was added to 250 μL of DMMB solution (21 mg of DMMB, 5 mL of absolute ethanol, and 2 mg of sodium formate per 1 L with pH adjusted to 1.5). The absorbance was then measured at 595 nm, and the amount of sHya was determined by comparing against a calibration curve.

To determine the surface morphology of aECM coated PANI substrates, the vacuum-dried substrates were sputtered with gold using 30 μA current for 30 s (Denton Vacuum, Desk V HP), and images

DOI: 10.1021/acsami.5b06390
ACS Appl. Mater. Interfaces 2015, 7, 23015−23028

were acquired at 20 kV in secondary electron mode by using a scanning electron microscope (SEM, FEI Inspect F20) equipped with an energy dispersive spectrometer (EDS) system to analyze the surface composition.

2.2.2. Conductivity Measurement. The conductivities of uncoated and aECM coated PANI substrates were measured by the four-probe technique using a DC probe station (Agilent Device Analyzer B1500A). A very small electrical contact was made using silver paste on all four corners of square samples before the measurement. A constant current was applied between two adjacent corners, and the voltage across the remaining two corners was measured to give resistance. The standard van der Pauw method[24] was employed for evaluating the sheet resistance of the films using the following equation:

$$e^{-\pi R_A/R_S} + e^{-\pi R_B/R_S} = 1$$

where R_A and R_B are the resistance values measured using the van der Pauw configuration from all the four sides of the sample. The required conductivity of the sample can then be determined from $\sigma = 1/R_s \times d$, where σ is the bulk conductivity in S/cm, and d is the sample thickness.

2.3. Electric Field Stimulated Cell Culture Experiments. Primary human MSCs from bone marrow aspirates of a healthy, 20-year-old male were kindly provided by Katrin Müller group Professor M. Bornhäuser, Medical Clinic I, Dresden University Hospital Carl Gustav Carus, with the approval from local ethics commission (ethic vote No. EK 263122004). This is a well-characterized and routinely used hMSC-line in our lab, which displayed insignificant differences in differentiation profile from other hMSCs (age between 20 and 40 years) (Supplementary Figures 1 and 2) and when used in pulsatile electrical stimulation experiments.[19,20] The isolated hMSCs were expanded in expansion media made up of Dulbecco's modified Eagle medium (DMEM) supplemented with 10% of fetal bovine serum (FBS), 2 mM L-glutamine, and 1% penicillin streptomycin (P/S) solution (Sigma, Germany) in an incubator with humidified atmosphere containing 5% CO_2 at 37 °C. Each set of electrical stimulation experiment was conducted independently and repeated thrice with hMSCs of passage 4.

Each film was seeded initially with 5×10^3 cells/cm^2 in 48-well plate for 24 h. Subsequently, the constructs were placed in the electrochambers with differentiation media containing the expansion media supplemented with 0.2 mM L-ascorbic acid, 10 nM dexamethasone, and 10 mM β-glycerolphosphate. Fresh differentiation media was replaced every 3 days. Since glass coverslips are inert to electrical fields and are commonly used in stem cells differentiation studies, we have used this (control/Coll) as the baseline to infer the efficacy of conductive PANI substrates to drive osteogenesis.

The electrochamber was based on the design model of Hess et al., which works on the principle of TLC.[21] The primary current was generated by a pulse generator (Type EMG 1153) in series with a linear amplifier (Type Kepco BOP 72−6M). The cellular constructs (control/Coll-PEF, PANI/Coll-PEF, and PANI/Coll/sHya-PEF) were subjected to rectangular pulses (7 ms, 3.6 mV/cm, 10 Hz) for durations of 4 h followed by a 4 h break (throughout the complete cultivation period of 28 days). The corresponding unstimulated samples (control/Coll, PANI/Coll, and PANI/Coll/sHya) were placed in identical chambers without applying electric fields. For biochemical assessment, three samples per group were taken from the chamber at defined time points, washed with PBS, and frozen at −80 °C until further analyses.

2.4. Cell Morphological Analysis Using Fluorescence Microscopy. The morphology of hMSCs after 3 days of PEF stimulation was assessed by fluorescence microscopy (Zeiss, Axio Obsever.Z1). The samples were fixed in 4% phosphate-buffered formalin, and the cells were permeabilized with 0.1% Triton X-100 in PBS (Sigma). After being washed twice with wash buffer (0.05% Tween-20 in PBS), the samples were incubated in blocking solution (1% BSA in PBS containing 0.05% Tween-20) for 30 min. Then the constructs were incubated at room temperature for 1 h in mouse antivinculin monoclonal antibody (Invitrogen, 1:150 dilution) followed by three washes in wash buffer for 5 min each. Further, the constructs were incubated with Alexa Fluor-488 goat antimouse secondary antibody (Invitrogen) for 1 h at a dilution of 1:250, followed by washing cells three times in wash buffer. To visualize the actin filaments, the cells were stained with Alexa Fluor-546 Phalloidin (Invitrogen, 1:50 dilution) for 20 min and counterstained with 4′,6-diamidino-2-phenylindole (DAPI) (Invitrogen, 1:1000 dilution) for 2 min to visualize the cell nuclei. The cell area was calculated by tracing the boundary of the cells in fluorescence image using free hand line tool in the ImageJ software. The surface area of at least 15 cells, chosen at random from each field, was measured.

2.5. Biochemical Assays. *2.5.1. LDH Assay.* The proliferation of hMSCs was assessed by Cytotoxicity Lactate Dehydrogenase (LDH) Detection Kit (Takara, France). Briefly, the frozen constructs were carefully thawed and lysed on ice in 400 μL of lysis buffer containing 1% TritonX-100 in PBS. From that, 50 μL of cell lysate was transferred to a 96-well plate and incubated with 50 μL of LDH substrate solution (room temperature, dark). The enzymatic reaction was terminated with 0.5 M HCl after 10 min, and the absorbance was measured immediately at 492 nm in a microplate reader (Tecan). LDH activity was correlated with cell number using a calibration curve of cell lysate with defined cell numbers.

2.5.2. DNA Content. The cellular DNA content was determined by the fluorometric quantification method using Quant-iT PicoGreen dsDNA Kit (Molecular Probes, Invitrogen). Ten microliters of cell lysate from each sample was mixed with DNA binding Picogreen dye solution at 1:800 dilution in Tris-EDTA-buffer (10 mM TRIS, 1 mM EDTA, pH 7.5) in a 96-well black plate. The fluorescent intensity of the mixed solution was measured after 5 min on a fluorescence spectrometer (Tecan). The calibration curve between the DNA and cell number was plotted by use of lysates with defined cell numbers.

2.5.3. ALP Activity. ALP activity was detected by a colorimetric method using p-nitrophenol assay, in which p-nitrophenylphosphate (pNPP), a colorless organic phosphate ester substrate, is converted to p-nitrophenol, a yellow colored product by the enzymatic action of ALP. In a 96-well plate, 25 μL of cell lysates was incubated at 37 °C for 30 min with 125 μL of 3.7 mM pNPP in substrate buffer (0.1 M diethanolamine, 1 mM $MgCl_2 \cdot 6H_2O$, and 0.1% Triton X-100, pH 9.8). The reaction was stopped by the addition of 65 μL of 1 N NaOH and was centrifuged at 3345g for 15 min. The absorbance of the supernatant was measured at 405 nm in a 96-well microplate reader (Tecan). The activity of ALP was normalized against the cell number.

2.5.4. Calcium Determination. Calcium concentration in the cell lysate was quantified colorimetrically using the O-Cresolphthalein Complexone Methodology (CPC liquicolor kit (Stanbio, TX)) according to the manufacturer's protocol. Calcium was extracted by incubating 96 μL of cell lysate overnight in 4 μL of 6 M HCl with gentle shaking. From this calcium extract, 10 μL was pipetted in a 96-well plate along with 350 μL of the base and color reagents added in 1:1 mixture, and the absorbance was measured immediately at 590 nm.

2.6. Gene Expression Analysis. Total RNA was isolated from the frozen samples after 1, 14, 21, and 28 days using TRIzol reagent (Invitrogen) according to the manufacturer's protocol. The isolated RNA was resuspended in nuclease-free water, and the concentrations were measured on a ND-1000 UV spectrophotometer (Nanodrop). cDNA synthesis was performed using Accuscript cDNA synthesis kit (Agilent), as per manufacturer instructions. About 500 ng of RNA per sample was used as the template for cDNA synthesis. Quantitative real-time PCR (qPCR) assays were then performed using Brilliant II SYBR Green QPCR low ROX Master Mix (Agilent) on a Mx3005P real-time PCR machine (Agilent Technologies, Waldbronn, Germany). Each PCR reaction mix contained 2 μL of cDNA per sample and a primer concentration of 200 nM. PCR amplification was achieved under the following parameters: initial denaturation at 95 °C for 10 min, followed by 40 cycles of denaturation at 95 °C for 30 s, annealing at 57−60 °C for 30 s, and extension at 72 °C for 30 s. At the end of the run, an additional melt curve step was included to ensure primer specificity. All samples were measured in triplicate, and to circumvent run-to-run variations, the entire samples for one particular gene were measured in a single qPCR run. Finally, the gene expression

DOI: 10.1021/acsami.5b06390
ACS Appl. Mater. Interfaces 2015, 7, 23015−23028

Table 1. Primer Sequence Used in the Real-Time PCR Analysis To Determine the Expression Level of Osteogenic Differentiation Markers (Referred from Hess et al.[22]). The Average of GAPDH and RPL13A Was Used as the Internal Control

	primer sequence			
genes	forward	reverse	amplicon Size (bp)	T_A in °C
RUNX-2	ACAGAACCACAAGTGCGGTGCA	TGCTTGCAGCCTTAAATGACTCTGT	128	58
ALPL	CGTCGATTGCATCTCTGGGCTCC	TGGTCTCGCCAGTACTTGGGGT	146	59
OCN	GAGCCCCAGTCCCCTACCC	GCCTCCTGAAAGCCGATGTG	103	59
OPN	TGATGGCCGAGGTGATAGTGTGGT	CCTGGGCAACGGGGATGG	161	60
COL1A1	AGACTGGCAACCTCAAGAAG	ACAGTGACGCTGTAGGTGAA	97	58
GAPDH	TGCACCACCAACTGCTTAGC	GGCATGGACTGTGGTCATGAG	87	60
RPL13A	CCTGGAGGAGAAGAGGAAAGAGA	TTGAGGACCTCTGTGTATTTGTCAA	126	60

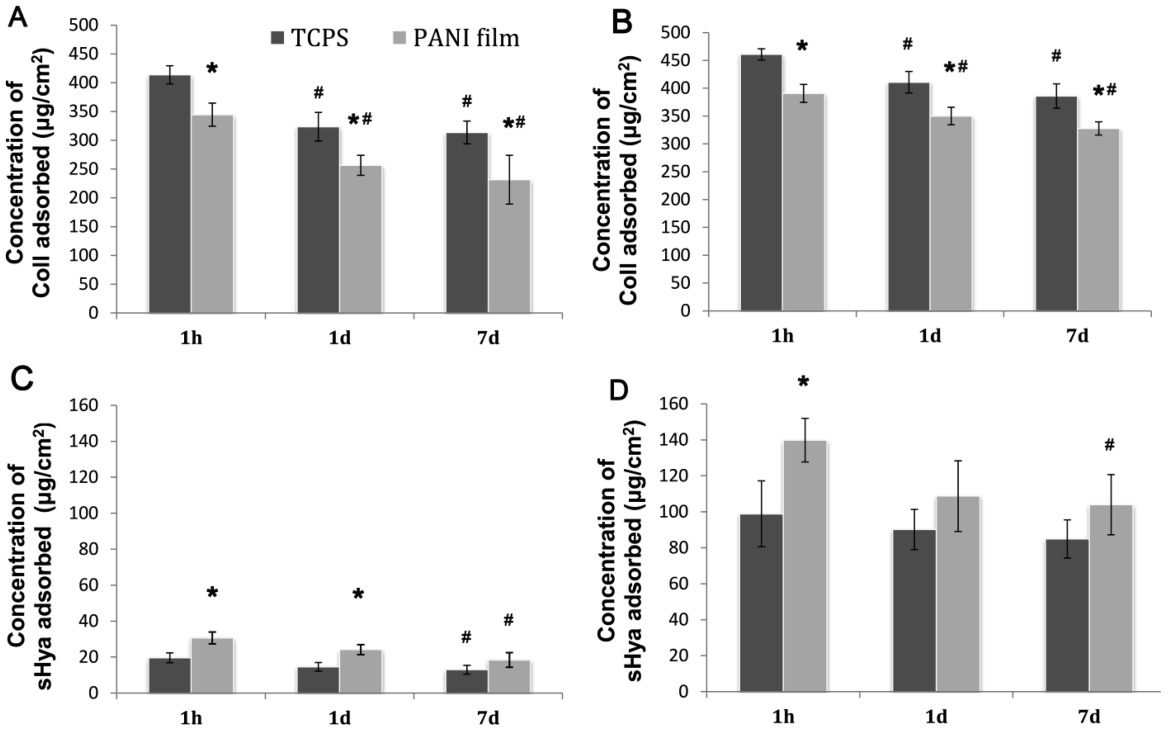

Figure 1. Stability of aECM coating on conductive substrate. Amount of immobilized collagen on (A) Coll coated and (B) Coll/sHya coated PANI and TCPS samples, respectively. Quantification of immobilized hyaluronic acid in (C) sHya coated and (D) Coll/sHya coated samples, respectively. Data represented as mean ± standard deviation (SD) of triplicates. Asterisk denotes statistically significant difference ($p < 0.05$) with respect to TCPS control at a given time point, and pound sign (#) indicates significant difference ($p < 0.05$) with respect to their counterpart at 1 h. Data points represent mean ± SD ($n = 4$).

data were analyzed by the well-established $2^{-\Delta\Delta Ct}$ method.[25] The gene expression data were normalized against the average of two reference genes, GAPDH and RPL13A, and expressed in fold ratio relative to the control coverslip (control/Coll) on day 1. The primers used for PCR are listed in Table 1.

2.7. Statistical Analysis. All data were represented as mean ± standard deviation. All experiments were repeated at least twice independently, with three replicates per sample. Statistical analysis was performed using one-way ANOVA and student's *t* test, and values of $p < 0.05$ were considered statistically significant.

3. RESULTS

3.1. Physico-Chemical Properties of aECM Coated PANI Matrices. *3.1.1. Stability Analysis of aECM Coating.* One of the essential requirements in biomimetic coating is to ensure stable bonding of biomolecules on material surface without compromising the bioactivity of the introduced biomolecule.[26] It is known that covalent immobilization procedures can deter the bioactivities of functional components of biomolecules.[27] In the present context, Coll and sHya were allowed to physisorb onto the polymeric surface, as physisorption of fibrillar proteins is known to result in almost stable immobilization.[28] To comparatively investigate the stability of individual aECM coatings on PANI, quantitative evaluation of desorption kinetics on PANI was compared against tissue culture polystyrene (TCPS), a typical standard used in the field, after immersion in PBS for three different time points of up to 7 days (Figure 1). Upon comparing the Coll content on PANI against TCPS control, a significantly higher amount of Coll was found on the control surface than the PANI surface. In addition, the profiles indicated an initial desorption over the first 24 h of incubation, after which a steady level was maintained. After 7 days of incubation in PBS, the amount of Coll immobilized on PANI was determined to be 231 ± 42 $\mu g/cm^2$ in the case PANI/Coll (Figure 1A) and 328 ± 11.9 $\mu g/cm^2$ in the case of PANI/Coll/sHya (Figure 1B). Hence, it is evident that the addition of sHya can improve the attachment and stability of collagen fibrils on PANI surface.

DOI: 10.1021/acsami.5b06390
ACS Appl. Mater. Interfaces 2015, 7, 23015−23028

In contrast, it is notable that more sHya was detected on PANI surface than on TCPS surface when immobilized either alone or with Coll (Figure 1C,D). Moreover, a markedly greater amount of sHya immobilization was noticed on PANI/Coll/sHya surface than on PANI/sHya substrates. Especially, the DMMB assay results showed a five-fold increase in sHya retention onto PANI surface when PANI/Coll/sHya was compared against PANI/sHya. Thus, sHya can be effectively immobilized in larger quantities when it is associated with Coll during fibrillogenesis than when adsorbed alone.

3.1.2. Morphological Features of aECM Coated PANI. The surface characteristics of the Coll and sHya coated PANI substrates were studied by scanning electron microscopy. The pristine PANI substrates exhibited a smooth surface topography with minor orifices, a result of solvent escaping from the bulk through the surface (Figure 2A). The PANI/sHya substrates

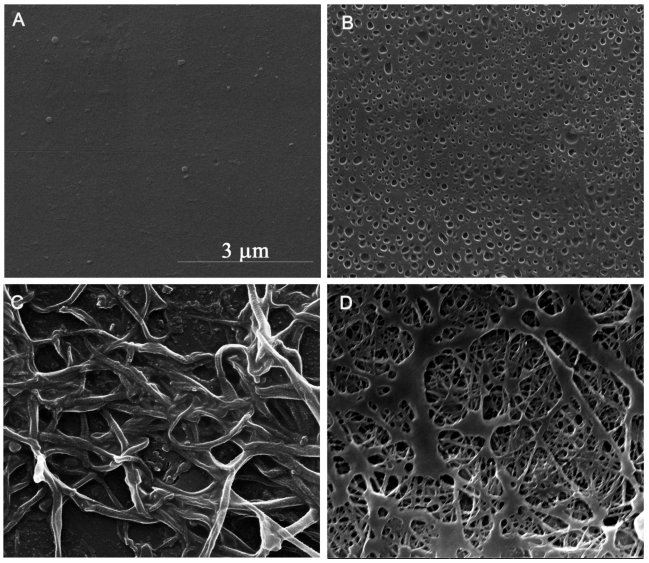

Figure 2. Surface characterization of aECM coated PANI matrices. SEM images of (A) Pristine PANI surface, (B) PANI/sHya, (C) PANI/Coll, and (D) PANI/Coll/sHya, respectively.

displayed a mesoporous surface topography with pore sizes ranging from 200−300 nm (Figure 2B). In contrast, PANI/Coll presented a random disarray of collagen fibers of 200−250 nm in diameter as a result of in vitro fibrillogenesis (Figure 2C). In the case of PANI/Coll/sHya substrates, the fibril diameter was found to be significantly smaller (80−100 nm) in comparison to PANI/Coll substrates (Figure 2D). Thus, the PANI/Coll/sHya film appears as a nanofibrous mat composed of collagen fibrils within micron-sized pores.

Given the information about the morphological features of the aECM coating, identification of the elemental composition was performed by energy dispersive X-ray spectrometry (EDS). The spectra were recorded from different regions of the aECM coated PANI substrates for analysis. The atom percents of the different elements detected by EDS have been listed in Table 2. It may be noted that nitrogen (N) signals were not recorded within the detection limits of the EDS detector. The decrease in the atom % of carbon (C) is commensurate to the increase in atom % of oxygen (O) arised from the coating molecules (Coll and sHya). In case of PANI/Coll, small amounts of Chlorine (Cl), Sodium (Na), and Phosphorus (P) along with Coll were adsorbed onto the substrates from the buffer solution, while no sulfur was detected. However, no P was detected in the PANI/sHya sample due to the presence of sulfate groups from sHya. The atom % of C was halved, while that of O was doubled in PANI/Coll/sHya. This can be expected from the greater amounts of Coll and sHya adsorbed onto PANI in the presence of each other as compared to their adsorption in isolation (Figure 1). Further, the enhanced adsorption of Coll and sHya in PANI/Coll/sHya has also led to a proportionate increase in the atom % of Cl, Na, S, and P. On the basis of the above results, it can be concluded that aECM coated PANI has ECM-like physicochemical characteristics.

3.1.3. Electrical Conductivities of PANI with Different aECM Coatings. It is known that any difference in the conductivity values of polymers is affected by the type of counterions of the dopant molecules, and this effect is mainly contributed by the increase in mobility of charge carriers in the conduction band.[29] As seen from the plot (Figure 3A), the uncoated samples had a conductivity of 10^{-8} S/cm, making them highly insulating substrates. On the other hand, coating with sHya (PANI/sHya) improved the conductivity to 10^{-5} S/cm due to the presence of sulfate and carboxylate groups, which act as the dopant moieties. An unexpectedly higher conductivity of 10^{-4} S/cm was obtained for PANI/Coll as compared to PANI/sHya. This may be due to the adsorption of additional acetate groups from the coating buffer onto the collagen triple helices. Further, a maximum conductivity of 10^{-3} S/cm was achieved on PANI/Coll/sHya. Such a trend in conductivity is also in agreement with the stable immobilization of these aECM molecules on the PANI/Coll/sHya substrates (Figure 1). This together with the incorporation of various ions from buffer solution confers enhanced conductivity to the polymeric chains (Table 2). Correspondingly, the current−voltage (I−V) curves of the coated PANI substrates showed an ohmic behavior, as shown in Figure 3, panel B, indicating an apparent decrease in polymer resistance with different dopant addition. Inconsistent readings of the voltage near zero current in uncoated PANI (Figure 3D) may be due to the difficulty in measuring small voltages.[30]

3.2. Influence of PEF Stimulation on Adhesion, Proliferation, and Osteogenesis of hMSCs on Conducting aECM Coated PANI Substrates. In this section, we present and analyze the results of adhesion, proliferation, and differentiation of hMSCs in osteogenic induction medium at

Table 2. Elemental Composition Analysis of aECM Coated PANI Substrates Determined by SEM/EDS

	elements (atom %)					
sample	C	O	S	Cl	Na	P
PANI	98.5 ± 0.5			1.5 ± 0.5		
PANI/Coll	74.5 ± 0.5	22.5 ± 0.2		1.6 ± 0.2	1.0 ± 0.2	0.4 ± 0.1
PANI/sHya	74.8 ± 2.4	22.2 ± 2.0	0.2 ± 0.1	1.7 ± 0.1	1.1 ± 0.3	
PANI/Coll/sHya	37.3 ± 7.4	47.9 ± 3.3	1.0 ± 0.3	4.1 ± 1.0	6.4 ± 0.3	3.3 ± 1.5

DOI: 10.1021/acsami.5b06390
ACS Appl. Mater. Interfaces 2015, 7, 23015−23028

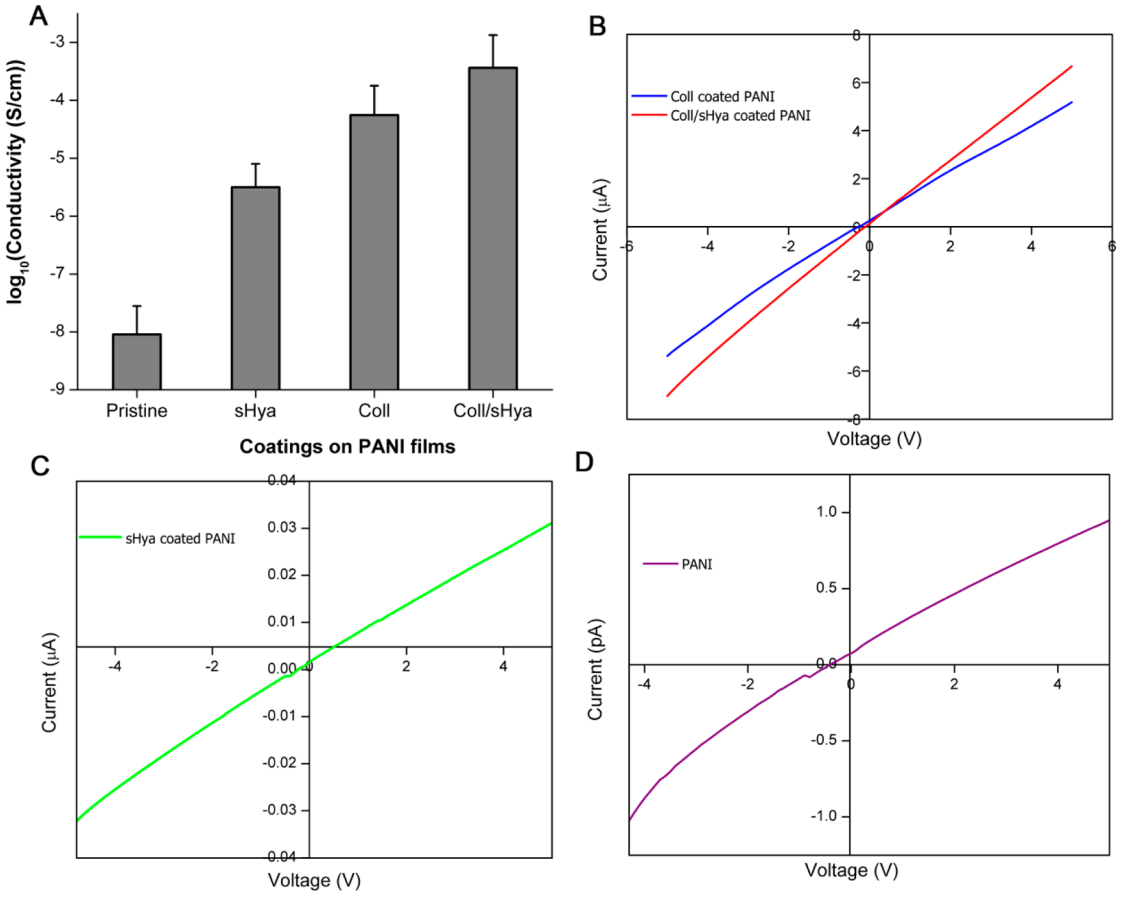

Figure 3. Electrical characterization of PANI with different coatings. (A) Graph showing the variable electrical conductivity of the PANI substrates with different coatings, determined by four point probe method. (B–D) *I*–*V* curves of PANI substrate coated with Coll (B, blue), Coll/sHya (B, red); (C) sHya coated PANI; and (D) noncoated pristine PANI films, respectively.

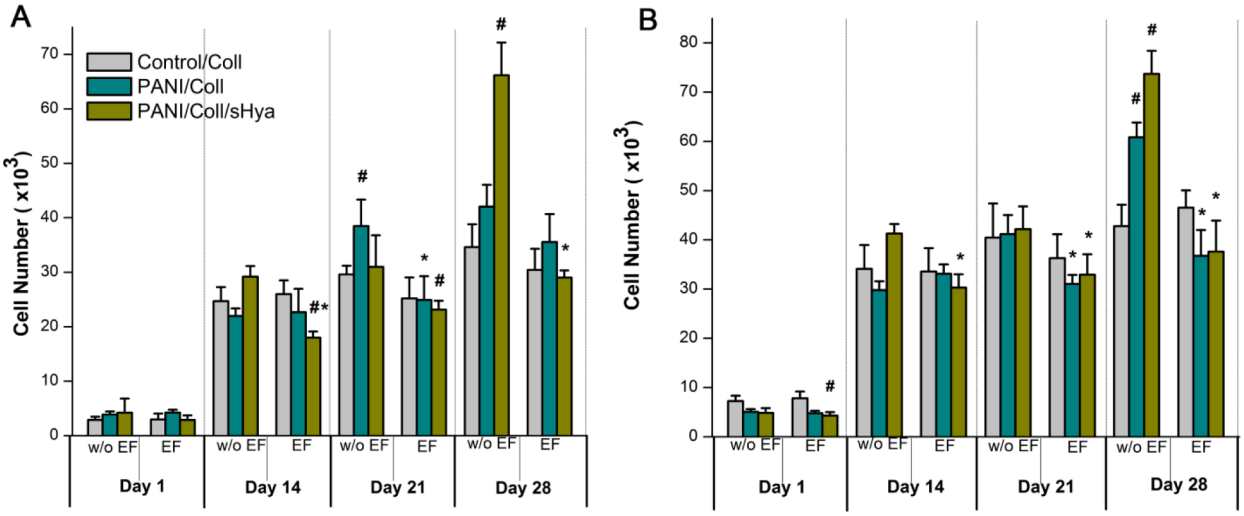

Figure 4. Effect of aECM coating and PEF stimulation on cell proliferation. (A) Graph showing number of metabolically active cells at regular time intervals in the presence and absence of PEF, as determined by LDH assay. (B) Total DNA content of cells, as quantified by picogreen assay. The results showed higher DNA content in untreated PANI/Coll/sHya substrates on day 28, in accordance with the LDH assay data, which show similar trend in cell number. Pound sign (#) denotes statistically significant difference ($p < 0.05$) with respect to untreated control at a given time point, and asterisk indicates significant difference ($p < 0.05$) between untreated and PEF treated samples at the given time point. Data points represent mean ± SD ($n = 3$).

various time points in culture. The TLC approach was adopted to deliver periodic stimulation (7 ms rectangular pulses, 3.6 mV/cm, 10 Hz) for 4 h with 4 h pause for up to 28 days.

3.2.1. Proliferative Behaviors of PEF Stimulated hMSCs. Cell proliferation in response to PEF exposure was evaluated by two complementary techniques, namely LDH and picogreen

DOI: 10.1021/acsami.5b06390
ACS Appl. Mater. Interfaces 2015, 7, 23015–23028

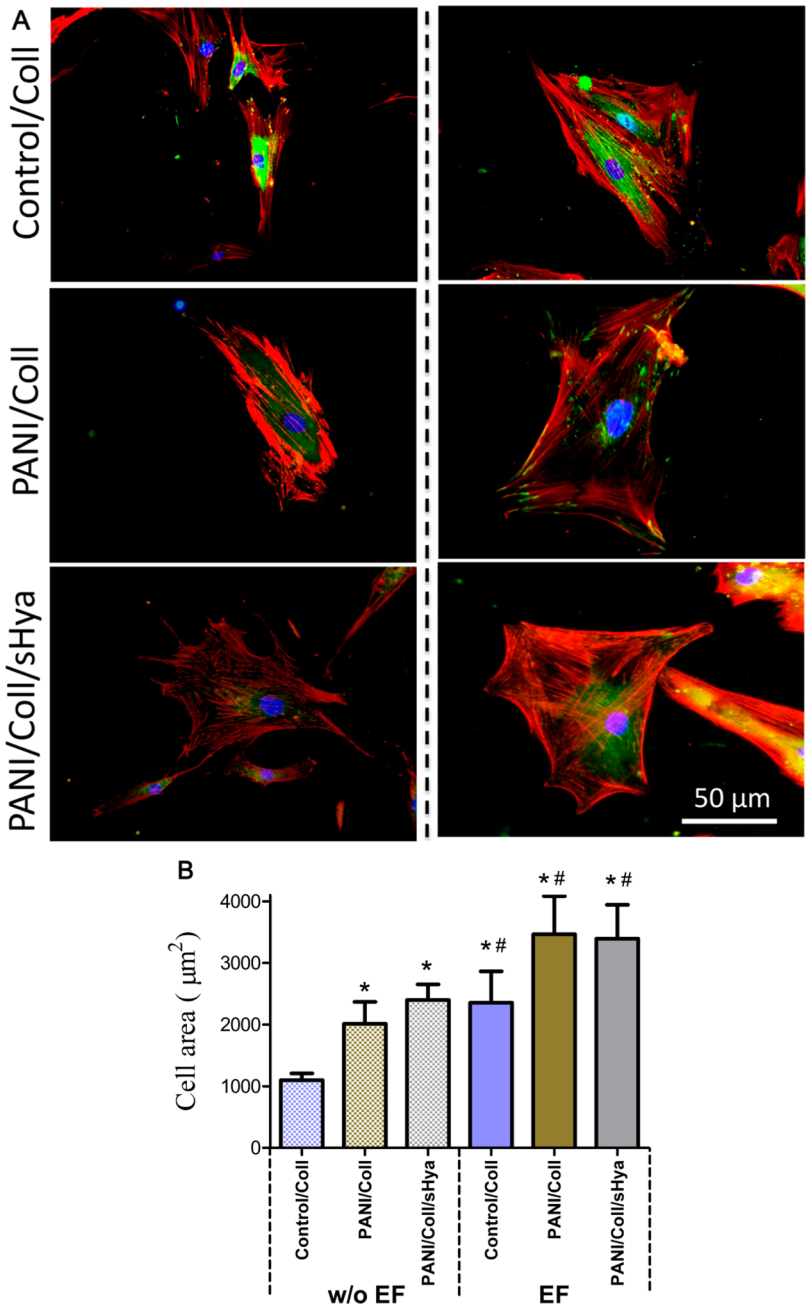

Figure 5. Cell morphology changes in response to underlying conductivity and PEF stimulation. (A) Shown are the merged fluorescence images of hMSCs grown on control/Coll, PANI/Coll, and PANI/Coll/sHya, respectively, without (left panels) and with (right panels) PEF stimulation. After culture for 3 days, hMSCs were processed for immunofluorescence with Alexa Fluor 568 phalloidin (red) to probe F-actin, antivinculin (green), and DAPI (blue). (B) Plot of the average cell spread area on various samples in the presence or absence of PEF stimulation. Asterisk denotes statistically significant difference ($p < 0.05$) with respect to nonstimulated control (control/Coll), and pound sign (#) indicates significant difference ($p < 0.05$) between untreated and PEF treated counterparts. All data are expressed as mean ± SD ($n \geq 15$) and are representative of at least three different samples.

assay. While LDH is based on metabolic activity, picogreen assay quantifies the total cellular DNA content. Thus, any variability in cellular metabolism due to PEF stimulation can be discerned by performing the additional fluorometric assay, which is more accurate in measuring the DNA content and hence cell proliferation.[31] Figure 4, panel A shows the proliferation profile of hMSCs over 28 days in culture with and without PEF stimulation, as determined by LDH assay. It is observed that PANI/Coll and PANI/Coll/sHya had a profound influence in significantly enhancing cell proliferation at a later stage, that is, on day 28. Notably, PANI/Coll/sHya marked the highest proliferation on day 28. In contrast, with PEF stimulation, the cell number was significantly lower than their nonstimulated counterparts, but was almost comparable to control/Coll.

The number of cells determined from picogreen assay exhibited the same trend as the cell number calculated from the LDH activity (Figure 4B). Particularly, proliferation was highly favored on PANI/Coll/sHya without PEF simulation, but the increase was not as remarkable as the one observed from the

DOI: 10.1021/acsami.5b06390
ACS Appl. Mater. Interfaces 2015, 7, 23015−23028

LDH assay. Collectively, the cell enumeration data from these two different assays illustrate that the PEF stimulation does not have additive or synergistic effects with aECM coating on the conducting matrices, in promoting cell proliferation. Rather, the presence of Coll and sHya on conducting substrates had only enriched the proliferative capacity of hMSCs at the later stage of culture (i.e., day 28).

3.2.2. Cytoskeleton Organization and Focal Adhesion of hMSCs on aECM Coated Substrates upon PEF Stimulation. We then compared substrate dependent morphological changes of hMSCs cultured with and without PEF stimulation. On control/Coll, hMSCs displayed spindle-shaped morphology with distinct actin cytoskeleton (Figure 5A). In parallel, hMSCs cultured on PANI/Coll or PANI/Coll/sHya exhibited a higher level of cell spreading. Besides, the cells appeared comparatively larger in size on PANI/Coll/sHya substrates to those on PANI/Coll substrates. Following PEF stimulation, both PANI/Coll and PANI/Coll/sHya substrates induced cell attachment with a more spread morphology and well organized cytoskeleton compared to their nonstimulated counterparts. Moreover, the adhesion occurred with the formation of mature focal adhesion points, as can be visualized from the vinculin staining. However, the focal adhesion points were more prominent and were slightly concentrated at the narrow cell edges in PEF stimulated PANI/Coll substrates when compared to PANI/Coll/sHya. To quantify these substantial differences in cell spreading, we computed the cross-sectional area of individual cells adhered on control as well as PANI substrates. The cells on PEF stimulated PANI substrates displayed larger surface areas than on other surfaces, as shown in Figure 5, panel B. Specifically, the cell area was 1.5−1.8-times greater in PEF stimulated hMSCs on PANI substrates compared to non-stimulated ones. However, there was no statistically significant difference in spread area between PEF stimulated PANI/Coll and PANI/Coll/sHya substrates. Overall, such a flattened and polygonal-shaped morphology of hMSCs on PEF stimulated PANI/Coll and PANI/Coll/sHya substrates, analogous to the features of osteoblasts indicate the early onset of differentiation on conducting substrates in the presence of PEF.

3.2.3. Accelerated ALP Activity in Conducting PANI/Coll/sHya Substrates upon PEF Stimulation. The activity of ALP, one of the early osteogenic markers, was evaluated to investigate the differentiation patterns of hMSCs cultured on conducting substrates under PEF stimulated growth conditions. As the typical characteristic nature of osteoblastic differentiation,[32] a temporal rise and fall in ALP activity was recorded in all experimental groups (Figure 6). Almost at each time point studied, the ALP activity was significantly higher in the PEF stimulated cultures, when compared to nonstimulated culture. With increasing time of culture, a progressive stepwise increment in the ALP activity was recorded in all the samples until 21 days of culture, whereas it declined gradually toward later time points. Especially, the highest level of ALP activity was recorded on PEF stimulated PANI/Coll/sHya substrates on day 21. It can be noted that the ALP level in nonstimulated group at day 21 was comparable to the PEF stimulated one at day 14, indicating a significant acceleration in osteogenesis by 1 week upon PEF exposure. Moreover, it is also apparent that the ALP activity in PEF stimulated hMSCs cultured on PANI/Coll was significantly increased to that in the control/Coll on day 14, which represents the conductivity dependent effect in eliciting early stage of osteogenesis.

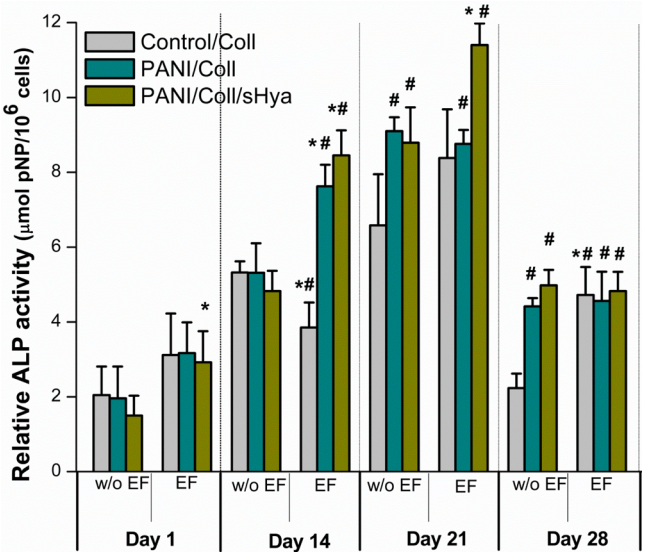

Figure 6. Effect of PEF treatment on ALP activity of hMSCs grown on conducting aECM coated substrates at different time points. Values were normalized to the total cell number (determined by LDH assay) for each individual sample. Pound sign (#) denotes statistically significant difference ($p < 0.05$) with respect to untreated control at a given time point, and asterisk indicates significant difference ($p < 0.05$) between untreated and PEF treated samples at the given time point. Data are shown as mean ± SD ($n = 3$) and represent results from three independent experiments.

3.2.4. Conducting Substrates Have Profound Effects in Elevating Calcium Concentrations under PEF Stimulated Culture Conditions. The concentration of calcium in each construct was quantified using CpC assay to evaluate the calcium phosphate deposition produced by differentiating hMSCs. Figure 7 depicts the calcium content normalized to hMSCs, grown on conducting substrates with corresponding aECM coatings in the presence and absence of PEF

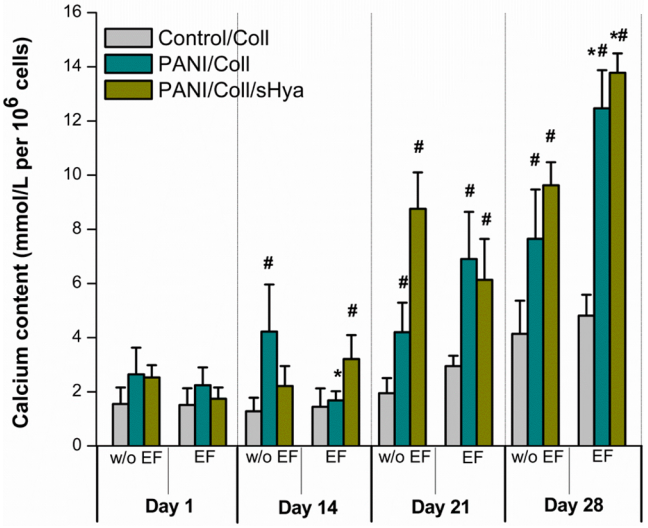

Figure 7. Total calcium content in osteogenic differentiated culture with or without PEF exposure at different time points. The amount of calcium was analyzed by cresolphthalein complexone calcium assay kit, and the data were normalized per cell number (determined by LDH assay) in each sample. #, $P < 0.05$ versus control; ∗, $P < 0.05$ versus untreated counterpart. The bars demonstrate the mean ± SD ($n = 3$).

DOI: 10.1021/acsami.5b06390
ACS Appl. Mater. Interfaces 2015, 7, 23015−23028

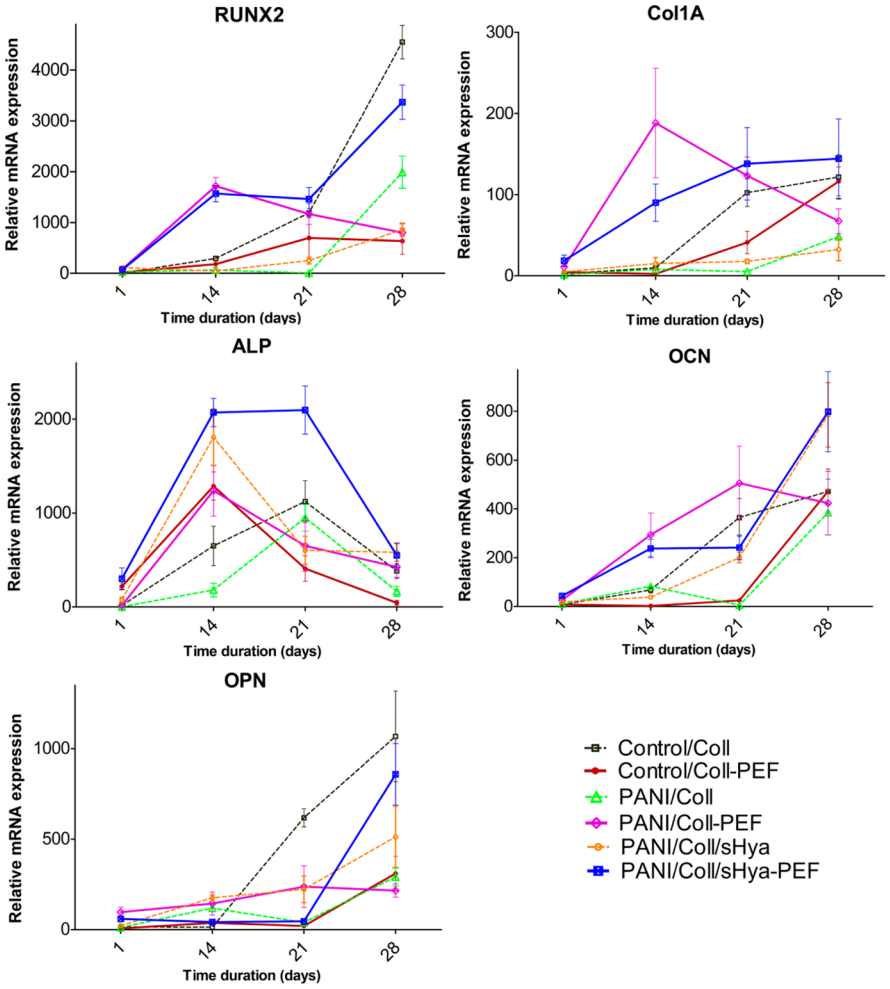

Figure 8. Gene expression profiles of bone markers suggesting the osteogenic conversion of hMSCs on conducting aECM coated substrates with and without PEF exposure. The expression of ALP and OCN was markedly increased upon PEF stimulation on conducting aECM substrates, while that of Col1A, RUNX2, and OPN was similar to that of the untreated control cells cultured in osteogenic medium. Results are representative of three independent experiments, and data expressed as mean ± SD, n = 3.

stimulation. The calcium level consistently increased over time, revealing the potential of the substrates to induce mineralization. Calcium concentrations on control substrates (control/Coll), with or without PEF stimulation, was found to be much lesser than on conducting substrates. The hMSCs on PANI/Coll/sHya substrates demonstrated similar or slightly higher calcium deposition when compared to the PANI/Coll substrates, and both showed much greater calcium deposition than control/Coll. At day 28, PEF stimulated PANI/Coll and PANI/Coll/sHya substrates had the highest calcium deposition, with an increase by 1.5-fold compared to other groups.

In general, the production of mineralized matrix is considered as the end point of osteoblast maturation.[34] Although PEF exposure did not have any apparent effect in inducing calcium deposition at early time points, it had a predominant influence on later osteoblastic differentiation, as characterized by enhanced calcium deposition at day 28. These results highlight the application of PEF in augmenting calcium deposition at the later time point of culture rather than at an early stage.

3.2.5. Dynamic Expression Profiles of Osteogenic Markers in PEF Stimulated hMSCs. To evaluate the combined effect of PEF stimulation and aECM coated PANI in promoting osteogenesis of hMSCs, the expression of five important bone related genes was evaluated by quantitative reverse trancriptase PCR (qRT-PCR). As shown in Figure 8, the data depicted that these five genes, namely Runt-related transcription factor 2 (*RUNX2*), Alkaline phosphatase (*ALP*), Collagen type 1, α 1 (*COL1A1*), Osteocalcin (*OCN*), and Osteopontin (*OPN*), elucidated a significant difference in expression between PEF stimulated and nonsimulated groups, with further variation in the data imparted by the type of aECM coating on the substrates. Figure 8 depicts the mRNA expression pattern of *RUNX2*, one of the early markers that indicate osteoblastic differentiation and bone formation.[33] A high level of *RUNX2* expression was recorded in hMSCs cultured on PANI/Coll and PANI/Coll/sHya substrates in the presence of PEF. However, a late but prominent upregulation was observed on hMSCs of control group (control/Coll) on day 28. Since an early elevation in *RUNX2* expression was detected for PANI/Coll/sHya substrates and to some extent in PANI/Coll substrates, it is apparent that PEF stimulation on sHya containing aECM played an enhancing role in switching the commitment of hMSCs toward osteogenic lineage.

In contrast to the increases observed for *RUNX2* mRNA level on day 28, a rapid upregulation in *Col1A1* mRNA expression was detected on day 14 in PEF stimulated PANI/Coll substrates, which subsequently lowered by days 21 and 28.

DOI: 10.1021/acsami.5b06390
ACS Appl. Mater. Interfaces 2015, 7, 23015−23028

Instead, there was a steady escalation in *Col1A1* expression for all other samples tested, hitting the highest point at day 28. Even so, no substantial increment in the mRNA levels was detected in unstimulated PANI/Coll and PANI/Coll/sHya substrates.

Among the genes studied, the changes in *ALP* expression over time are most noteworthy, especially in PEF stimulated PANI/Coll/sHya substrates. Its mRNA expression peaked on day 14, which remained elevated on day 21 and dropped four-fold by day 28. Moreover, such a sharp increase was also observed in unstimulated PANI/Coll/sHya substrates on day 14, indicating that sHya plays a role in facilitating osteoblastic differentiation independent of PEF stimulation. Interestingly, the *ALP* transcript levels on PEF stimulated control/Coll and PANI/Coll groups on day 14 were almost comparable to those of their untreated counterparts on day 21. These data imply the accelerated upregulation of *ALP* transcripts, upon PEF stimulation, a process which is otherwise delayed by 7 days in their untreated counterparts. Importantly, the decreased *ALP* expression on day 28 confirms the commencement of terminal differentiation in hMSCs in all groups examined.

An analysis of the expression profile of *OCN* mRNA has indicated increased expression level by several fold in all batches examined during the late stages of culture, except for a slight discrepancy in PEF stimulated PANI/Coll substrates. *OCN* is secreted at the late stage of osteoblast maturation,[35] and its marked increment exclusively in both PEF stimulated and nonstimulated PANI/Coll/sHya substrates depicted the strong indication of terminal differentiation. In addition, the onset of early OCN expression at day 14, exclusively in PEF stimulated PANI/Coll and PANI/Coll/sHya, indicates that substrate conductivity could enhance early osteoblastic differentiation. As for *OPN* gene, only the control (control/Coll) substrates could induce an early expression on day 21 and day 28. Despite a relatively attenuated expression level in all other groups, PEF stimulated PANI/Coll/sHya substrates could trigger a delayed yet similar effect as the control group on day 28. On the whole, from the gene expression profile described, it is evident that the culture of hMSCs on aECM coated conducting matrices in the presence of PEF can remarkably enhance osteogenesis, with the additional advantage of shortening the time span taken for the differentiation process.

4. DISCUSSION

Among the various physical stimuli applied in modulating stem cell differentiation, the concept of using electric fields as an instructive cue to induce directed differentiation is considered as an attractive strategy.[34] The main goal of this study is to examine the independent or combinatory effect of aECM coating, substrate conductivity, or PEF stimulation in regulating the proliferation, morphology, and differentiation of hMSCs.

4.1. Coating of PANI Substrates and Influence of Coatings on Substrate Conductivity. In the present work, we have adopted the method of mimicking ECM-like microenvironment to develop biomimetic conducting platforms. Instead of the conventional covalent tethering of ECM molecules onto the substrates, we performed the physisorption process so that these biomolecules can serve as the substrate dopant, enabling improved conductivity. Apart from imparting substrate conductivity, it also establishes a biochemical environment with defined presentation of ECM molecules to provide surface-based control over the proliferation and differentiation of cultured hMSCs. It is also believed that the interactions of biologically active components with cells can be strengthened by immobilizing biomolecules on a surface in close proximity with their receptors on the cell membrane, rather than dispersing them as soluble signals in the culture medium, where they are less likely to encounter their targets.[35] Moreover, large dopant molecules such as sHya tend to get integrated in the polymer backbone effectively, avoiding leaching of the dopant with time and with the application of electrical stimulus.[13] Especially in our case, the highly conjugated backbone of polycationic PANI readily associated with the negatively charged sHya, and hence a higher amount of sHya was immobilized on PANI surface than on TCPS control (Figure 1C,D).

Defined microenvironments were created by coating PANI surface with ECM molecules, in particular with Coll and sHya, mimicking the composition of the organic ECM of bone. SEM images of the aECM coated PANI substrates clearly show a mesoporous coating in PANI/sHya (Figure 2B), a random disarray of thick collagen fibers in PANI/Coll (Figure 2C), and a nanofibrous coating in PANI/Coll/sHya due to reduced fibril growth in vitro (Figure 2D). Typically, fibrillogenesis occurs in two stages: nucleation, followed by growth of fibrils from tropocollagen triple helices.[36] Collagen fibrillogenesis is known to be markedly altered in the presence of glycosaminoglycans in vivo.[28] From the smaller fibril diameter observed in case of PANI/Coll/sHya, it is clear that sHya inhibited the growth of tropocollagen nucleating sites by competitive adsorption.

The electrical behavior of the aECM coated PANI substrates in our case is dictated by two parameters: (i) aECM composition or coating morphology and (ii) amount of adsorbed dopant ions/molecules. The experimentally observed order of conductivity is as follows: PANI/Coll/sHya > PANI/Coll > PANI/sHya > PANI (Figure 3A). Here, we provide a rationale for the observed conductivity in terms of the above-mentioned parameters. The higher abundance of porosity in the PANI/sHya makes it less conducting than PANI/Coll, which is also influenced by the meager amounts of sHya adsorption onto PANI surfaces (Figure 1C). On the contrary, the presence of additional phosphate and acetate (~10 mM) groups adsorbed from the buffer make PANI/Coll more conductive. In PANI/Coll/sHya, the electrical conductivity increased few orders of magnitude in comparison to pristine PANI and single component coatings (Coll or sHya alone). This is obvious from the greater amounts of the Coll and sHya immobilized onto PANI films (Figure 1B,D) along with a proportionate increase in the presence of other negatively charged dopant groups such as CH_3COO^-, Cl^-, and PO_4^{3-} (Table 2). Thus, Coll and sHya synergistically improved the electrical conductivity of PANI/Coll/sHya substrates.

4.2. Influence of aECM Coating and Substrate Conductivity on Cellular Behavior in the Absence of PEF Stimulation. Along with electrical conductivity, cellular behavior is also strongly influenced by aECM coating on PANI substrates. In particular, we show that PANI/Coll/sHya substrates promoted proliferation to a greater extent in the absence of PEF stimulation (Figure 4). This clearly illustrates the complementary influence of both substrate conductivity and sHya incorporation in promoting cell growth. The enhanced proliferative effect of sHya in the present study is in contrary to earlier studies, which demonstrated a reduction in cell proliferation on similarly coated nonconducting substrates.[37,38] Such a disparity in the observed effect may be reasoned in that sHya is concealed within the polymeric chains

DOI: 10.1021/acsami.5b06390
ACS Appl. Mater. Interfaces 2015, 7, 23015−23028

of PANI as a negative dopant. This can be inferred from the low atom % of sulfur in comparison to other elements detected by SEM-EDS (Table 2), a surface-sensitive technique. Furthermore, a seemingly subtle change in the multivalent hyaluronan ligand on PANI matrices can affect the interaction with its cellular receptors, which is implicated in mediating proliferation.[39] Moreover, multiple other factors can be responsible for the increased proliferative behavior observed in repeated and independent experiments on day 28. One factor concerns accelerated cell differentiation under PEF stimulated conditions hinders proliferation observed for conditions without PEF stimulation. A second factor can be traced back to cell morphology. From the morphological quantification of cross-sectional cell area, we noted an increase in the space covered by cells exclusively on PEF stimulated PANI substrates. This spatial constraints imposed by spread neighboring cells in PEF-stimulated group might be a possible reason that limit cell proliferation at a later stage in culture (i.e., on day 28). Indeed, several experimental and theoretical studies have been proposed that physical parameters, such as cell geometry or area, can regulate cell division and cell cycle progression.[40]

With regard to differentiation, the presence of sHya in the aECM coating had no significant effect on ALP activity but had a positive effect in increasing calcium ion content and osteocalcin expression on days 21 and 28, respectively. On comparing nonstimulated PANI/Coll with control/Coll, a relatively higher level of ALP activity and calcium accumulation was recorded on conducting PANI/Coll than on insulating control/Coll, on day 21 and 28, suggesting the role of conductivity in later stage of differentiation (Figures 6 and 7). In contrast, there was no improvement in gene expression of bone specific markers on conducting PANI substrates (PANI/Coll) with respect to insulating control/Coll in the absence of PEF. This implies that a combination of aECM coating and substrate conductivity does not accentuate osteogenic differentiation as effectively as that on their PEF stimulated counterparts (discussed in subsequent section).

4.3. Influence of aECM Coating and Substrate Conductivity on Cellular Behavior in the Presence of PEF Stimulation. The combinatorial effect of PEF stimulation and aECM coated conducting substrate on stem cell behavior is discussed in this section. In the presence of PEF stimulation, there was no detectable improvement in proliferation on aECM coated PANI substrates. This result on the growth behavior of hMSC is consensus to the report by Hammerick et al.,[41] wherein they did not detect any effect of PEF stimulation on the proliferation of mouse adipose derived stromal cells during a 10-day culture. Moreover, when subjected to PEF stimuli, the cells underwent distinguishable changes in their morphology with respect to their control (Figure 5A). The PEF stimulated hMSCs appeared larger in size with star-shaped morphology on conducting PANI substrates than on control coverslips (control/Coll), further supporting the role of underlying conductivity and aECM coating in the modulation of the cell morphology (Figure 5A). The adhesion of a cell to a substrate is mediated by the assembly of focal adhesion complexes (integrin-talin-vinculin-actin link) and the associated cytoskeleton. However, we found that the vinculin localization at the focal adhesion points is less predominant in PEF stimulated PANI/Coll/sHya compared to PANI/Coll, despite a well-spread morphology. These observations are consistent with those reported recently by Choi et al.,[42] who proposed based on simple electrostatic calculations that cells grown on conductive substrates may strongly adhere to the substrate without focal-adhesion complex formation, owing to the enhanced electrostatic interaction between cells and the substrate. In fact, the adhesion strengthening response is mainly enhanced by integrin binding and clustering, whereas vinculin recruitment has comparatively lesser contribution toward adhesion strength.[43] Furthermore, morphometric quantification of the changes in the cell spreading revealed greater cell area when grown on PANI/Coll and PANI/Coll/sHya substrates in the presence of PEF stimulation (Figure 5B). The variation observed in the cell spread area and morphology on PEF stimulated PANI/Coll/sHya substrates, exhibited signs of decreased proliferation at a later stage in culture (Figure 4), due to the spatial hindrance developed by largely spread cells.

Characteristically, cell morphological alterations are suggested to be a key regulator of MSC commitment. Similarly in our case, the PEF induced physical cues would have caused the assembly and disassembly of actin cytoskeleton, thereby regulating osteogenic differentiation.[44] It is also implicated that electrical stimulus alters the local electrical fields of ECM molecules, leading to the electrophoretic redistribution of cell surface receptors, thus influencing cell behavior.[45] Kotwal et al. elucidated an increase in fibronectin protein adsorption with electrical stimulation as the possible reason for enhanced neurite outgrowth on polypyrrole surfaces.[46]

The efficacy of pulsed electromagnetic fields in augmenting mRNA expression of osteogenic marker genes during differentiation and mineralization is widely elucidated by several research groups.[47,48] However, the superposition of magnetic field along with electric field generates different cellular effects compared to the one induced by electric field alone. Hence, the current study employs the approach of pulsed electric field stimulation by a transformer-like coupling technique, which eliminates the unwanted interference by magnetic fields or biochemical reactions at stimulating electrodes.[21] Apart from exploiting this noninvasive cell stimulation approach, the study was broadly inclined to better understand the participation of aECM coated conducting substrates in promoting osteogenesis. As a main finding, our results demonstrate a marked rise in gene expression of *ALP* and *OCN* in response to PEF stimuli on conducting PANI/Coll/sHya substrates (Figure 8). It is of note that control/Coll substrates that are electrically inert seemed to lack the ability to accelerate the upregulation of *ALP* and *OCN* genes, unlike conducting PANI/Coll and PANI/Coll/sHya. Both of these genes are known to play important roles in bone matrix synthesis and mineralization, respectively.[49] Similar up-regulation in *OCN* and *ALP* marker genes was noticed by Akhouayri et al.[50] upon exposing the cells to static mechanical stresses. In accordance with these results, Tanaka et al.[51] reported an increase in *OCN* expression exclusively by mechanically stimulating the cells using sinusoidal strain combined with broad frequency vibration.[52]

Likewise, we also observed that PEF exposure has stimulated significantly higher ALP activity (Figure 6) and calcium deposition (Figure 7) in a manner dependent on substrate conductivity. The transcription and protein expression of *ALP* is recognized as one of the key player in the early stage of osteogenesis.[53] At least one of its important roles is to initiate mineral deposition, as proved by studies in which inhibition of ALP activity blocked the mineralization process.[54−56] Similarly, our results support the same concept of greater calcium accumulation for PEF stimulated PANI/Coll/sHya samples by

DOI: 10.1021/acsami.5b06390
ACS Appl. Mater. Interfaces 2015, 7, 23015−23028

day 28 contributed by earlier onset of ALP activity over the first 21 days (Figures 6 and 7). Since the mineralization occurs in a cyclic manner and does not continue indefinitely, ALP activity had declined after 28 days in all samples. Calcium accumulation is considered as an essential phenotypic marker of the final stage of osteogenic differentiation.[57−59] An exceptionally higher extent of calcium accumulation (Figure 7) and osteocalcin expression in PEF exposed PANI/Coll/sHya substrates (Figure 8) confirmed the sign of osteoblast maturation and mineralization in hMSCs. Overall, when grown on aECM coated conducting substrates, hMSCs responded by alteration in their morphology, upregulation of specific osteogenic marker genes, and induce earlier onset of ALP activity along with calcium accumulation under PEF stimulated culture conditions (Figure 9).

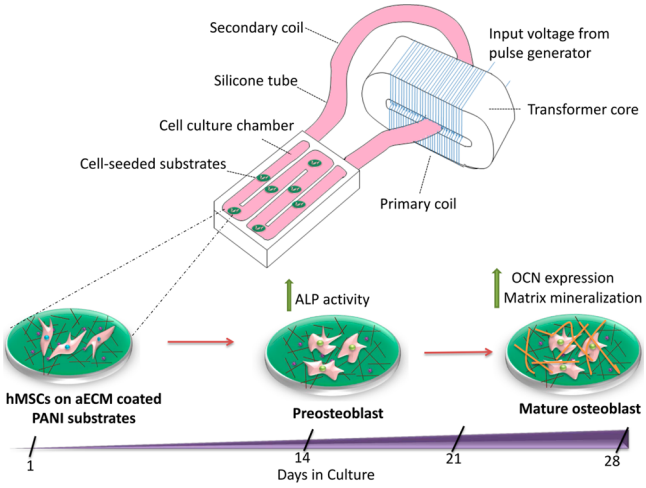

Figure 9. Schematic illustration of the TLC induced PEF stimulation of hMSCs cultured on aECM coated conducting PANI substrates, depicting the temporal progression of osteogenic differentiation.

In summary, our earlier work demonstrated the effect of substrate conductivity in combination with direct current electric stimuli in inducing hMSC differentiation toward neural-like lineage on PANI substrates.[60] On the other hand, the present study elucidates the interactive effects of aECM coated conducting PANI substrates and PEF stimulation in promoting osteogenic differentiation of hMSCs. All these combined results highlight the attractive strategy of manipulating cellular microenvironment to selectively guide the growth and commitment of stem cells.

5. CONCLUSIONS

Overall, the present study signifies the effectiveness of aECM coated conducting substrates and noninvasive PEF stimulated culture methodologies as interactive cues in inducing osteoblast differentiation of human bone marrow derived mesenchymal stem cells. These findings deepen our basic understanding of governing stem cell differentiation by tuning the matrix conductivity and electric field dosing. Altogether, these results collectively emphasizes the following points.

(a) The incorporation of sHya in aECM coated PANI substrates via in vitro fibrillogenesis enhanced the proliferative capacity of hMSCs but was ineffective in inducing differentiation in the absence of PEF.

(b) The underlying substrate conductivity exhibited a positive influence on ALP activity and calcium ion content at later time points (i.e., on day 21 and 28) when compared to nonstimulated control.

(c) PEF stimulation promoted early osteogenesis with a marked acceleration in ALP activity on conducting aECM coated PANI substrates, with additional enhancement induced by sHya on day 21. Moreover, higher calcium ion content was also observed on conducting PANI substrates irrespective of aECM composition.

(d) Differentiating hMSC populations displayed an intensified mRNA expression level for ALP and OCN, on sHya containing PANI (PANI/Coll/sHya) substrates in PEF stimulated culture conditions, in comparison to their nonstimulated counterparts.

Taken together, these evidences can shed light on the development of "smart" platforms by integrating well-controlled physicochemical cues and optimal stimulation modalities to regulate stem cell behavior for a variety of tissue engineering applications.

■ ASSOCIATED CONTENT

Supporting Information

The Supporting Information is available free of charge on the ACS Publications website at DOI: 10.1021/acsami.5b06390.

Antigen profiles of hMSC from different donors; comparison of multipotent differentiation behavior of hMSC from different donors (PDF)

■ AUTHOR INFORMATION

Corresponding Authors

*E-mail: Dieter.Scharnweber@tu-dresden.de.
*E-mail: bikram@mrc.iisc.ernet.in.

Author Contributions

⊥These authors contributed equally.

Notes

The authors declare no competing financial interest.

■ ACKNOWLEDGMENTS

The authors would like to thank the DFG German Research Council for support from the Transregio 67, projects A2 and A3. One of the authors, G.T. acknowledges travel grant support from Boehringer Ingelheim Fonds (BIF), Germany. G.T. also thank the lab-members of Prof. Dieter Scharnweber for their kind cooperation in facilitating the speedy completion of the work, as well as Dr. Matthias Schnabelrauch of Innovent e.V who had kindly provided the sHya used in this study. G.T. is grateful to Prof. Giridhar Madras (Chem Engg, IISc) for the extended support and supervision. The authors G.T. and B.B. would also like to acknowledge "Translational Center on Biomaterials for Orthopedic and Dental Applications" Department of Biotechnology (DBT), Government of India for financial assistance. The author P.L.S. would like to thank the DAAD for the Ph.D. scholarship.

■ REFERENCES

(1) Willerth, S. M.; Sakiyama-Elbert, S. E. Combining Stem Cells and Biomaterial Scaffolds for Constructing Tissues and Cell Delivery. In *StemBook*; Harvard Stem Cell Institute: Cambridge, MA, 2008.

(2) Amini, A. R.; Laurencin, C. T.; Nukavarapu, S. P. Bone Tissue Engineering: Recent Advances and Challenges. *Crit. Rev. Bioeng.* **2012**, *40*, 363−408.

DOI: 10.1021/acsami.5b06390
ACS Appl. Mater. Interfaces 2015, 7, 23015−23028

(3) Faia-Torres, A. B.; Guimond-Lischer, S.; Rottmar, M.; Charnley, M.; Goren, T.; Maniura-Weber, K.; Spencer, N. D.; Reis, R. L.; Textor, M.; Neves, N. M. Differential Regulation of Osteogenic Differentiation of Stem Cells on Surface Roughness Gradients. *Biomaterials* **2014**, *35*, 9023−9032.
(4) Yourek, G.; McCormick, S. M.; Mao, J. J.; Reilly, G. C. Shear Stress Induces Osteogenic Differentiation of Human Mesenchymal Stem Cells. *Regener. Med.* **2010**, *5*, 713−724.
(5) Lee, J.; Abdeen, A. A.; Kilian, K. A. Rewiring Mesenchymal Stem Cell Lineage Specification by Switching the Biophysical Microenvironment. *Sci. Rep.* **2014**, *4*, 1−8.
(6) Khetan, S.; Guvendiren, M.; Legant, W. R.; Cohen, D. M.; Chen, C. S.; Burdick, J. A. Degradation-Mediated Cellular Traction Directs Stem Cell Fate in Covalently Crosslinked Three-Dimensional Hydrogels. *Nat. Mater.* **2013**, *12*, 458−465.
(7) McNamara, L. E.; McMurray, R. J.; Biggs, M. J.; Kantawong, F.; Oreffo, R. O.; Dalby, M. J. Nanotopographical Control of Stem Cell Differentiation. *J. Tissue Eng.* **2010**, *1*, 120623.
(8) Lim, K.; Hexiu, J.; Kim, J.; Seonwoo, H.; Cho, W. J.; Choung, P. H.; Chung, J. H. Effects of Electromagnetic Fields on Osteogenesis of Human Alveolar Bone-Derived Mesenchymal Stem Cells. *BioMed Res. Int.* **2013**, *2013*, 1.
(9) McCullen, S. D.; McQuilling, J. P.; Grossfeld, R. M.; Lubischer, J. L.; Clarke, L. I.; Loboa, E. G. Application of Low-Frequency Alternating Current Electric Fields Via Interdigitated Electrodes: Effects on Cellular Viability, Cytoplasmic Calcium, and Osteogenic Differentiation of Human Adipose-Derived Stem Cell. *Tissue Eng., Part C* **2010**, *16*, 1377−1386.
(10) Hronik-Tupaj, M.; Rice, W. L.; Cronin-Golomb, M.; Kaplan, D. L.; Georgakoudi, I. Osteoblastic Differentiation and Stress Response of Human Mesenchymal Stem Cells Exposed to Alternating Current Electric Fields. *BioMed. Eng. OnLine.* **2011**, *10*, 9.
(11) Schemitsch, E. H.; Kuzyk, P. R. T. The Science of Electrical Stimulation Therapy for Fracture Healing. *Indian J. Orthop.* **2009**, *43*, 127−131.
(12) Haddad, J. B.; Obolensky, A. G.; Shinnick, P. The Biologic Effects and the Therapeutic Mechanism of Action of Electric and Electromagnetic Field Stimulation on Bone and Cartilage: New Findings and a Review of Earlier Work. *J. Altern. Complement Med.* **2007**, *13*, 485−490.
(13) Balint, R.; Cassidy, N. J.; Cartmell, S. H. Conductive polymers: Towards a Smart Biomaterial for Tissue Engineering. *Acta Biomater.* **2014**, *10*, 2341−2353.
(14) Ghasemi-Mobarakeh, L.; Prabhakaran, M. P.; Morshed, M.; Nasr-Esfahani, M. H.; Baharvand, H.; Kiani, S.; Al-Deyab, S. S.; Ramakrishna, S. Application of Conductive Polymers, Scaffolds and Electrical Stimulation for Nerve Tissue Engineering. *J. Tissue Eng. Regener. Med.* **2011**, *5*, e17−35.
(15) Li, L.; et al. Electrical Stimuli Improve Osteogenic Differentiation Mediated by Aniline Pentamer and PLGA Nanocomposites. *Biomed. Rep.* **2013**, *1*, 428−432.
(16) Becker, D.; Geissler, U.; Hempel, U.; Bierbaum, S.; Scharnweber, D.; Worch, H.; Wenzel, K. W. Proliferation and Differentiation of Rat Calvarial Osteoblasts on Type I Collagen-coated Titanium Alloy. *J. Biomed. Mater. Res.* **2002**, *59*, 516−527.
(17) Stadlinger, B.; Hintze, V.; Bierbaum, S.; Moller, S.; Schulz, M. C.; Mai, R.; Kuhlisch, E.; Heinemann, S.; Scharnweber, D.; Schnabelrauch, M.; Eckelt, U. Biological Functionalization of Dental Implants with Collagen and Glycosaminoglycans - A Comparative Study. *J. Biomed. Mater. Res., Part B* **2012**, *100B*, 331−341.
(18) Kliemt, S.; Lange, C.; Otto, W.; Hintze, V.; Moller, S.; von Bergen, M.; Hempel, U.; Kalkhof, S. Sulfated Hyaluronan Containing Collagen Matrices Enhance Cell Matrix-Interaction, Endocytosis, and Osteogenic Differentiation of Human Mesenchymal Stromal Cells. *J. Proteome Res.* **2013**, *12*, 378−389.
(19) Hess, R.; Neubert, H.; Seifert, A.; Bierbaum, S.; Hart, D. A.; Scharnweber, D. A Novel Approach for In Vitro Studies Applying Electrical Fields to Cell Cultures by Transformer-Like Coupling. *Cell Biochem. Biophys.* **2012**, *64*, 223−232.
(20) Hess, R.; Jaeschke, A.; Neubert, H.; Hintze, V.; Moeller, S.; Schnabelrauch, M.; Wiesmann, H. P.; Hart, D. A.; Scharnweber, D. Synergistic Effect of Defined Artificial Extracellular Matrices and Pulsed Electric Fields on Osteogenic Differentiation of Human MSCs. *Biomaterials* **2012**, *33*, 8975−8985.
(21) Ramamurthy, P. C.; Mallya, A. N.; Joseph, A.; Harrell, W. R.; Gregory, R. V. Synthesis and Characterization of High Molecular Weight Polyaniline for Organic Electronic Applications. *Polym. Eng. Sci.* **2012**, *52* (8), 1821−1830.
(22) Hintze, V.; Moeller, S.; Schnabelrauch, M.; Bierbaum, S.; Viola, M.; Worch, H.; Scharnweber, D. Modifications of Hyaluronan Influence the Interaction with Human Bone Morphogenetic Protein-4 (hBMP-4). *Biomacromolecules* **2009**, *10*, 3290−3297.
(23) Hempel, U.; Hintze, V.; Moller, S.; Schnabelrauch, M.; Scharnweber, D.; Dieter, P. Artificial Extracellular Matrices Composed of Collagen I and Sulfated Hyaluronan with Adsorbed Transforming Growth Factor β1 Promote Collagen Synthesis of Human Mesenchymal Stromal Cells. *Acta Biomater.* **2012**, *8*, 659−666.
(24) Van der Pauw, L. J. A Method of Measuring Specific Resistivity and Hall Effect of Discs of Arbitrary Shape. *Philips Res. Rep.* **1958**, *13*, 1−9.
(25) Schmittgen, T. D.; Livak, K. J. Analyzing Real-Time PCR Data by the Comparative C(T) Method. *Nat. Protoc.* **2008**, *3* (6), 1101−1108.
(26) Ao, H.; Xie, Y.; Tan, H.; Yang, S.; Li, K.; Wu, X.; Zheng, X.; Tang, T. Fabrication and In Vitro Evaluation of Stable Collagen/Hyaluronic Acid Biomimetic Multilayer on Titanium Coatings. *J. R. Soc., Interface* **2013**, *10* (84), 20130070.
(27) Huang, Y.; Luo, Q.; Li, X.; Zhang, F.; Zhao, S. Fabrication and In Vitro Evaluation of the Collagen/Hyaluronic Acid PEM Coating Crosslinked with Functionalized RGD Peptide on Titanium. *Acta Biomater.* **2012**, *8*, 866−877.
(28) Miron, A.; Rother, S.; Huebner, L.; Hempel, U.; Kappler, I.; Moeller, S.; Schnabelrauch, M.; Scharnweber, D.; Hintze, V. Sulfated Hyaluronan Influences the Formation of Artificial Extracellular Matrices and the Adhesion of Osteogenic Cells. *Macromol. Biosci.* **2014**, *14* (12), 1783−1794.
(29) Ateh, D. D.; Navsaria, H. A.; Vadgama, P. Polypyrrole-Based Conducting Polymers and Interactions with Biological Tissues. *J. R. Soc., Interface* **2006**, *3*, 741−752.
(30) Catedral, M. D.; Tapia, A. K. G.; Sarmago, R. V.; Tamayo, J. P.; Rosario, E. J. d. Effect of Dopant Ions on the Electrical Conductivity and Microstructure of Polyaniline (Emeraldine Salt). *Science Diliman* **2004**, *16*, 41.
(31) Quent, V. M.; Loessner, D.; Friis, T.; Reichert, J. C.; Hutmacher, D. W. Discrepancies Between Metabolic Activity and DNA Content as Tool to Assess Cell Proliferation in Cancer Research. *J. Cell Mol. Med.* **2010**, *14*, 1003−1013.
(32) Bancroft, G. N.; Sikavitsas, V. I.; van den Dolder, J.; Sheffield, T. L.; Ambrose, C. G.; Jansen, J. A.; Mikos, A. G. Fluid Flow Increases Mineralized Matrix Deposition in 3D Perfusion Culture of Marrow Stromal Osteoblasts in a Dose-Dependent Manner. *Proc. Natl. Acad. Sci. U. S. A.* **2002**, *99* (20), 12600−12605.
(33) Sila-Asna, M.; Bunyaratvej, A.; Maeda, S.; Kitaguchi, H.; Bunyaratavej, N. Osteoblast Differentiation and Bone Formation Gene Expression in Strontium-inducing Bone Marrow Mesenchymal Stem Cell. *Kobe J. Med. Sci.* **2007**, *53*, 25−35.
(34) Monici, M.; Cialdai, F. In *Tissue Regeneration—From Basic Biology to Clinical Application*; Davies, J., Ed.; InTech: Rijeka, Croatia, 2012; Chapter 1, pp 13−34.
(35) Mashayekhan, S.; Miyazaki, J. In *Methodological Advances in the Culture, Manipulation, and Utilization of Embryonic Stem Cells for Basic and Practical Applications*; Atwood, C., Ed.; InTech: Rijeka, Croatia, 2011; Chapter 6, pp 93−112.
(36) Douglas, T.; Heinemann, S.; Mietrach, C.; Hempel, U.; Bierbaum, S.; Scharnweber, D.; Worch, H. Interactions of Collagen Types I and II with Chondroitin Sulfates A-C and Their Effect on Osteoblast Adhesion. *Biomacromolecules* **2007**, *8* (4), 1085−1092.

DOI: 10.1021/acsami.5b06390
ACS Appl. Mater. Interfaces 2015, 7, 23015−23028

(37) Wojak-Cwik, I. M.; Hintze, V.; Schnabelrauch, M.; Moeller, S.; Dobrzynski, P.; Pamula, E.; Scharnweber, D. Poly(L-lactide-co-glycolide) Scaffolds Coated with Collagen and Glycosaminoglycans: Impact on Proliferation and Osteogenic Differentiation of Human Mesenchymal Stem Cells. *J. Biomed. Mater. Res., Part A* **2013**, *101* (11), 3109−3122.
(38) Hintze, V.; Miron, A.; Moller, S.; Schnabelrauch, M.; Heinemann, S.; Worch, H.; Scharnweber, D. Artificial Extracellular Matrices of Collagen and Sulphated Hyaluronan Enhance the Differentiation of Human Mesenchymal Stem Cells in the Presence of Dexamethasone. *J. Tissue Eng. Regener. Med.* **2014**, *8* (4), 314−324.
(39) Ahrens, T.; Assmann, V.; Fieber, C.; Termeer, C.; Herrlich, P.; Hofmann, M.; Simon, J. C. CD44 is the Principal Mediator of Hyaluronic-Acid-Induced Melanoma Cell Proliferation. *J. Invest. Dermatol.* **2001**, *116* (1), 93−101.
(40) Streichan, S. J.; Hoerner, C. R.; Schneidt, T.; Holzer, D.; Hufnagel, L. Spatial Constraints Control Cell Proliferation in Tissues. *Proc. Natl. Acad. Sci. U. S. A.* **2014**, *111* (15), 5586−5591.
(41) Hammerick, K. E.; James, A. W.; Huang, Z.; Prinz, F. B.; Longaker, M. T. Pulsed Direct Current Electric Fields Enhance Osteogenesis in Adipose-Derived Stromal Cells. *Tissue Eng., Part A* **2010**, *16* (3), 917−931.
(42) Choi, W. J.; Jung, J.; Lee, S.; Chung, Y. J.; Yang, C. S.; Lee, Y. K.; Lee, Y. S.; Park, J. K.; Ko, H. W.; Lee, J. O. Effects of Substrate Conductivity on Cell Morphogenesis and Proliferation Using Tailored, Atomic Layer Deposition-Grown ZnO Thin Films. *Sci. Rep.* **2015**, *5*, 9974.
(43) Gallant, N. D.; Michael, K. E.; Garcia, A. s. J. Cell Adhesion Strengthening: Contributions of Adhesive Area, Integrin Binding, and Focal Adhesion Assembly. *Mol. Biol. Cell* **2005**, *16* (9), 4329−4340.
(44) Born, A. K.; Rottmar, M.; Lischer, S.; Pleskova, M.; Bruinink, A.; Maniura-Weber, K. Correlating Cell Architecture with Osteogenesis: First Steps Towards Live Single Cell Monitoring. *Eur. Cell Mater.* **2009**, *18*, 49−62.
(45) Patel, N.; Poo, M. M. Orientation of Neurite Growth by Extracellular Electric Fields. *J. Neurosci.* **1982**, *2*, 483−496.
(46) Kotwal, A.; Schmidt, C. E. Electrical Stimulation Alters Protein Adsorption and Nerve Cell Interactions with Electrically Conducting Biomaterials. *Biomaterials* **2001**, *22* (10), 1055−1064.
(47) Chang, W. H.; Chen, L. T.; Sun, J. S.; Lin, F. H. Effect of Pulse Burst Electromagnetic Field Stimulation on Osteoblast Cell Activities. *Bioelectromagnetics* **2004**, *25*, 457−465.
(48) Tsai, M. T.; Li, W. J.; Tuan, R. S.; Chang, W. H. Modulation of Osteogenesis in Human Mesenchymal Stem Cells by Specific Pulsed Electromagnetic Field Stimulation. *J. Orthop. Res.* **2009**, *27*, 1169−1174.
(49) Plant, A.; Tobias, J. H. Characterisation of the Temporal Sequence of Osteoblast Gene Expression During Estrogen-Induced Osteogenesis in Female Mice. *J. Cell. Biochem.* **2001**, *82*, 683−691.
(50) Akhouayri, O.; Lafage-Proust, M. H.; Rattner, A.; Laroche, N.; Caillot-Augusseau, A.; Alexandre, C.; Vico, L. Effects of Static or Dynamic Mechanical Stresses on Osteoblast Phenotype Expression in Three-Dimensional Contractile Collagen Gels. *J. Cell. Biochem.* **2000**, *76*, 217−230.
(51) Tanaka, S. M.; Li, J.; Duncan, R. L.; Yokota, H.; Burr, D. B.; Turner, C. H. Effects of Broad Frequency Vibration on Cultured Osteoblasts. *J. Biomech.* **2003**, *36*, 73−80.
(52) Liedert, A.; Kaspar, D.; Augat, P.; Ignatius, A.; Claes, L. In *Mechanosensitivity in Cells and Tissues*; Kamkin, A, Kiseleva, I., Eds.; Academia: Moscow, 2005.
(53) Birmingham, E.; Niebur, G. L.; McHugh, P. E.; Shaw, G.; Barry, F. P.; McNamara, L. M. Osteogenic Differentiation of Mesenchymal Stem Cells is Regulated by Osteocyte and Osteoblast Cells in a Simplified Bone Niche. *Eur. Cell Mater.* **2012**, *23*, 13−27.
(54) Golub, E. E.; Boesze-Battaglia, K. The Role of Alkaline Phosphatase in Mineralization. *Curr. Opin. Orthop.* **2007**, *18*, 444−448.
(55) Bellows, C. G.; Aubin, J. E.; Heersche, J. N. Initiation and Progression of Mineralization of Bone Nodules Formed In Vitro: the Role of Alkaline Phosphatase and Organic Phosphate. *Bone Miner.* **1991**, *14* (1), 27−40.
(56) Genge, B. R.; Sauer, G. R.; Wu, L. N.; McLean, F. M.; Wuthier, R. E. Correlation Between Loss of Alkaline Phosphatase Activity and Accumulation of Calcium During Matrix Vesicle-Mediated Mineralization. *J. Biol. Chem.* **1988**, *263* (34), 18513−18519.
(57) Owen, T. A.; Aronow, M.; Shalhoub, V.; Barone, L. M.; Wilming, L.; Tassinari, M. S.; Kennedy, M. B.; Pockwinse, S.; Lian, J. B.; Stein, G. S. Progressive Development of the Rat Osteoblast Phenotype In Vitro: Reciprocal Relationships In Expression of Genes Associated with Osteoblast Proliferation and Differentiation During Formation of the Bone Extracellular Matrix. *J. Cell. Physiol.* **1990**, *143* (3), 420−430.
(58) Ji, Z.; Cheng, Y.; Yuan, P.; Dang, X.; Guo, X.; Wang, W. Panax Notoginseng Stimulates Alkaline Phosphatase Activity, Collagen Synthesis, and Mineralization in Osteoblastic MC3T3-E1 cells. *In Vitro Cell. Dev. Biol.: Anim.* **2015**, *23*, 1−8.
(59) Xynos, I. D.; Hukkanen, M. V.; Batten, J. J.; Buttery, L. D.; Hench, L. L.; Polak, J. M. Bioglass 45S5 Stimulates Osteoblast Turnover and Enhances Bone Formation In Vitro: Implications and Applications for Bone Tissue Engineering. *Calcif. Tissue Int.* **2000**, *67* (4), 321−329.
(60) Thrivikraman, G.; Madras, G.; Basu, B. Intermittent Electrical Stimuli For Guidance of Human Mesenchymal Stem Cell Lineage Commitment Towards Neural-Like Cells on Electroconductive Substrates. *Biomaterials* **2014**, *35* (24), 6219−6235.

DOI: 10.1021/acsami.5b06390
ACS Appl. Mater. Interfaces 2015, 7, 23015−23028